ATPC: Adaptive Transmission Power Control for Wireless Sensor Networks

SHAN LIN, Stony Brook University
FEI MIAO, University of Pennsylvania
JINGBIN ZHANG, University of Virginia
GANG ZHOU, College of William and Mary
LIN GU, NingBo ShuFang Information Tecknology Co., Ltd.
TIAN HE, University of Minnesota
JOHN A. STANKOVIC and SANG SON, University of Virginia
GEORGE J. PAPPAS, University of Pennsylvania

Extensive empirical studies presented in this article confirm that the quality of radio communication between low-power sensor devices varies significantly with time and environment. This phenomenon indicates that the previous topology control solutions, which use static transmission power, transmission range, and link quality, might not be effective in the physical world. To address this issue, online transmission power control that adapts to external changes is necessary. This article presents ATPC, a lightweight algorithm for Adaptive Transmission Power Control in wireless sensor networks. In ATPC, each node builds a model for each of its neighbors, describing the correlation between transmission power and link quality. With this model, we employ a feedback-based transmission power control algorithm to dynamically maintain individual link quality over time. The intellectual contribution of this work lies in a novel pairwise transmission power control, which is significantly different from existing node-level or network-level power control methods. Also different from most existing simulation work, the ATPC design is guided by extensive field experiments of link quality dynamics at various locations over a long period of time. The results from the real-world experiments demonstrate that (1) with pairwise adjustment, ATPC achieves more energy savings with a finer tuning capability, and (2) with online control, ATPC is robust even with environmental changes over time.

Categories and Subject Descriptors: C.2.2 [**Computer-Communication Networks**]: Network Protocols

General Terms: Design, Algorithms, Performance

Additional Key Words and Phrases: Adaptive control, feedback, link quality, sensor network, transmission power control

6

This work is supported by the National Science Foundation, under NSF grants CNS-1239108, CNS-1218718, CNS-0931239, IIS-1231680, and CNS-1253506 (CAREER). We would like to thank Professor Gang Tao, Professor Lionel M. Ni, and anonymous reviewers for their insightful comments.
Authors' addresses: S. Lin, Department of Electrical and Computer Engineering, Stony Brook University, Stony Brook, NY 11001; email: shan.x.lin@stonybrook.edu; F. Miao and G. J. Pappas, Department of Electrical and Systems Engineering, University of Pennsylvania, Philadelphia, PA 19104; emails: {miaofei, pappasg}@seas.upenn.edu; J. Zhang, Department of Computer Science, University of Virginia, Charlottesville, VA 19103; email: jz7q@virginia.edu; G. Zhou, Computer Science Department, College of William and Mary, Williamsburg, VA 23185; email: gzhou@cs.wm.edu; L. Gu, NingBo ShuFang Information Technology Co., Ltd., Hong Kong; email: lingu@d-thinker.org; T. He, Computer Science Department, University of Minnesota, Minneapolis, MN, 55455; email: tianhe@cs.umn.edu; J. A. Stankovic and S. Son, Computer Science Department, University of Virginia, Charlottesville, VA 22904; emails: {stankovic, son}@cs.virginia.edu.

DOI: http://dx.doi.org/10.1145/2746342

ACM Reference Format:
Shan Lin, Fei Miao, Jingbin Zhang, Gang Zhou, Lin Gu, Tian He, John A. Stankovic, Sang Son, and George J. Pappas. 2016. ATPC: Adaptive transmission power control for wireless sensor networks. ACM Trans. Sen. Netw. 12, 1, Article 6 (March 2016), 31 pages.
DOI: http://dx.doi.org/10.1145/2746342

1. INTRODUCTION

With the integration of sensing and communication abilities in tiny devices, wireless sensor networks are widely deployed in a variety of environments, supporting military surveillance [Arora et al. 2004; Liu et al. 2003], emergency response [Xu et al. 2004; Liu et al. 2010], medical care [Stankovic et al. 2005; Asare et al. 2012], and scientific exploration [Tolle et al. 2005]. The in situ impact from these environments, together with energy constraints of the nodes, makes reliable and efficient wireless communication a challenging task. Under a constrained energy supply, reliability and efficiency are often at odds with each other. Reliability can be improved by transmitting packets at the maximum transmission power [He et al. 2004; Werner-Allen et al. 2006], but this situation introduces unnecessarily high energy consumption. To provide system designers with the ability to dynamically control the transmission power, popularly used radio hardware such as CC1000 [ChipconCC1000 2005] and CC2420 [ChipconCC2420 2005] offers a register to specify the transmission power level during runtime. It is desirable to specify the minimum transmission power level that achieves the required communication reliability for the sake of saving power and increasing the system lifetime.

Although theoretical study and simulation provide a valuable and solid foundation, solutions found by such efforts may not be effective in real running systems. Simplified assumptions can be found in these studies, for example, static transmission power, static transmission range, and static link quality. These studies do not consider the spatial-temporal impact on wireless communication. In this article, we present systematic studies on these impacts. There are a number of empirical studies on communication reality conducted with real sensor devices [Zhao and Govindan 2003; Woo et al. 2003; Zhou et al. 2004; Cerpa et al. 2005; Reijers et al. 2004; Lal et al. 2003]. Their results suggest that for a specified transmission power and communication distance, the received signal power varies and the link quality is unstable. But they do not focus on a systematic study of the radio and link dynamics in the context of different transmission power settings. Our extensive experiments with MICAz [CROSSBOW 2004] confirm the observations presented in previous work. We also go further and explore the radio and link dynamics when different transmission power levels are applied. Our experimental results identify that link quality changes differently according to spatial-temporal factors in a real sensor network. To address this issue, we design a pairwise transmission power control. Our empirical study also reveals that it is feasible to choose a minimal and environment-adapting transmission power level to save power while guaranteeing specified link quality at the same time.

To achieve the optimal power consumption for specified link qualities, we propose ATPC, an adaptive transmission power control algorithm for wireless sensor networks. The result of applying ATPC is that every node knows the proper transmission power level to use for each of its neighbors, and every node maintains good link qualities with its neighbors by dynamically adjusting the transmission power through on-demand feedback packets. Uniquely, ATPC adopts a feedback-based and pairwise transmission power control. By collecting the link quality history, ATPC builds a model for each neighbor of the node. This model represents an in situ correlation between transmission power levels and link qualities. With such a model, ATPC tunes the transmission power according to monitored link quality changes. The changes of transmission power

level reflect changes in the surrounding environment. ATPC supports packet-level transmission power control at runtime for MAC and upper layer protocols. For example, routing protocols with transmission power as a metric [Singh et al. 1998; Subbarao 1999; Gomez et al. 2003; Ganesan et al. 2001; Chipara et al. 2006] can make use of ATPC by choosing the route with optimal power consumption to forward packets.

The topic of transmission power control is not new, but our approach is quite unique. In state-of-the-art research, many transmission power control solutions use a single transmission power for the whole network, not making full use of the configurable transmission power provided by radio hardware to reduce energy consumption. We refer to this group as network-level solutions, and typical examples in this group are Park and Sivakumar [2002b], Narayanaswamy et al. [2002], Bettstetter [2002], Kirousis et al. [2000], and Santi and Blough [2003]. Also, some other work takes the configurable transmission powers into consideration. They assume either that each node chooses a single transmission power for all the neighbors [Bettstetter 2002; Kirousis et al. 2000; Kubisch et al. 2003; Ramanathan and R-Hain 2000; Wattenhofer et al. 2001; Kawadia et al. 2001; Park and Sivakumar 2002a; Rodoplu and Meng 1999; Li et al. 2002], which we refer to as node-level solutions, or that nodes use different transmission powers for different neighbors [Liu and Li 2002; Xue and Kumar 2004; Blough et al. 2003], which we call neighbor-level solutions. While these solutions provide a solid foundation for our research, ATPC goes further to support packet-level transmission power control in a pairwise manner.

Also, most existing real wireless sensor network systems use a network-level transmission power for each node, such as in He et al. [2004] and Werner-Allen et al. [2006]. These coarse-level power controls lead to high energy consumption. The authors of Son et al. [2004] present a valuable study about the impact of variable transmission power on link quality. Through our empirical experiments with the MICAz platform, it is observed that different transmission powers are needed to achieve the same link quality over time. This leads to our feedback-based transmission power control design, which is not addressed in Son et al. [2004]. Also, Son et al. [2004] use a fixed number of transmission powers (13 levels), which fixes the maximum accuracy for power tuning. The ATPC we propose chooses different transmission power levels based on the dynamics of link quality, and it also allows for better tuning accuracy and more energy savings. Our approach essentially represents a good tradeoff between accuracy and cost, a finer control at each node in exchange for less energy consumption when transmitting the packets.

In this work, we invest a fair amount of effort to obtain empirical results from three different sites and over a reasonably long time period. These results give practical guidance to the overarching design of ATPC. We demonstrate that ATPC greatly extends the system lifetime by choosing a proper transmission power for each packet transmission, without jeopardizing the quality of data delivery. In our 3-day experiment with 43 MICAz motes, ATPC achieves above a 98% end-to-end Packet Reception Ratio in the natural environment through fair and rainy days. The solutions without online tuning can barely deliver half of packets. Compared to other solutions, ATPC also significantly saves transmission power. With equivalent communication performance, ATPC only consumes 53.6% of the transmission energy of the maximum transmission power solution and 78.8% of the transmission energy of the network-level transmission power solution. More specifically, the contributions of our work lie in two aspects:

—Our systematic study and experiments reveal the spatiotemporal impacts on wireless communication and identify the relationship between the dynamics of link quality and transmission power control.
—With runtime pairwise transmission power control, we achieve a high packet delivery ratio successfully with small energy consumption under realistic scenarios.

The rest of this article is organized as follows: the motivation of this work is presented in Section 2. In Section 3, the design of ATPC is stated. In Section 4, ATPC is evaluated in real-world experiments. The state of the art is analyzed in Section 5. In Section 6, conclusions are given and future work is pointed out.

2. MOTIVATION

Radio communication quality between low-power sensor devices is affected by spatial and temporal factors. The spatial factors include the surrounding environment, such as terrain, and the distance between the transmitter and the receiver. Temporal factors include surrounding environmental changes in general, such as weather conditions. In this section, we present experimental results for investigation of these impacts. We note that previous empirical studies on communication reality [Zhao and Govindan 2003; Cerpa et al. 2005; Zhou et al. 2004; Ganesan et al. 2002; Reijers et al. 2004; Lal et al. 2003] suggest that for a specified transmission power, fixed communication distance, and antenna direction, the received signal power and the link quality vary. But they do not focus on a systematic study of the radio and link dynamics when different transmission powers are considered. We conducted these measurements, and we are the first to study systematically the spatial and temporal impacts on the correlation between transmission power and Received Signal Strength Indicator (RSSI)/Link Quality Indicator (LQI) [IEEE 802.15.4 1999]. Both RSSI and LQI are useful link metrics provided by CC2420 [ChipconCC2420 2005]. RSSI is a measurement of signal power that is averaged over eight symbol periods of each incoming packet. LQI is a measurement of the "chip error rate" [ChipconCC2420 2005], which is also implemented based on samples of the error rate for the first eight symbols of each incoming packet. The transmission power level index refers to the value specified for the RF output power provided by CC2420 [ChipconCC2420 2005]. It can be mapped to output power in units of dBm.

Our empirical results show that link quality is significantly influenced by spatiotemporal factors, and that every link is influenced to a different degree in a real system. This observation proves that the assumptions made from previous work about the static impact of the environment on link quality do not hold. Solutions based on these simplifying assumptions may not accurately capture the dynamics of communication quality, and may result in highly unstable communication performance in real wireless sensor networks. Therefore, the in situ transmission power control is essential for maintaining good link quality in reality.

2.1. Investigation of Spatial Impact

To investigate the spatial impact, we study the correlation between transmission power and link qualities in three different environments: a parking lot, a grass field, and a corridor, as shown in Figure 1. We use one MICAz as the transmitter and a second MICAz as the receiver. They are put on the ground at different locations, maintaining the same antenna direction. The transmitter sends out 100 packets (20 packets per second) at each transmission power level. The receiver records the average RSSI, the average LQI, and the number of packets received at each transmission power level. The experiments are repeated with five different pairs of motes in the same environmental conditions to obtain statistical confidence.

Figure 2 shows our experimental data obtained from one pair of nodes in different environments. Each curve demonstrates the correlation between the transmission power and RSSI/LQI at a certain distance of that pair. The confidence intervals (97%) of RSSI/LQI are also plotted on Figure 2. Clearly, there is a strong correlation between transmission power level and RSSI/LQI. We note that there is an approximately linear correlation between transmission power and RSSI in Figures 2(a), 2(c), and 2(e). The

(a) Experiments on a Grass Field

(b) Experiments in a Parking Lot

(c) Experiments in a Corridor

Fig. 1. Experimental sites.

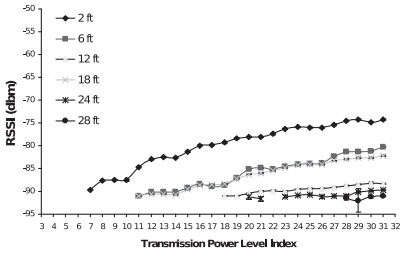

(a) RSSI Measured on a Grass Field

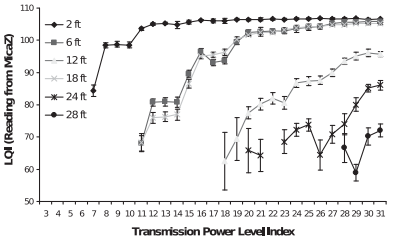

(b) LQI Measured on a Grass Field

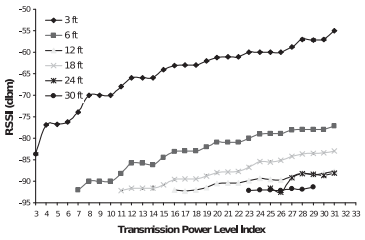

(c) RSSI Measured in a Parking Lot

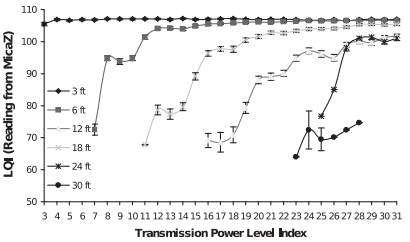

(d) LQI Measured in a Parking Lot

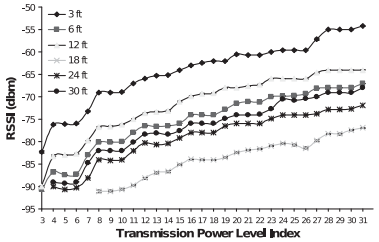

(e) RSSI Measured in a Corridor

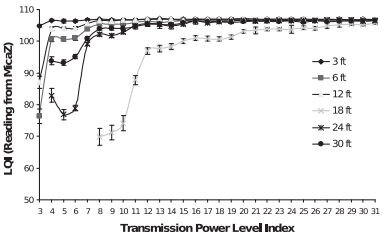

(f) LQI Measured in a Corridor

Fig. 2. Transmission power versus RSSI/LQI at different distances in different environments.

LQI curves in Figures 2(b), 2(d), and 2(f) also present approximately linear correlations when the LQI readings are small. However, the LQI readings suffer saturation when they get close to 110, which is the maximum quality frame detectable by the CC2420 [ChipconCC2420 2005]. We also notice that each LQI curve and its corresponding RSSI curve demonstrate similar trends and variations. This is because the LQI reading is

also a representation of the SNR value, which is the ratio of the received signal power level to the background noise level.

The slopes of RSSI curves generally decrease as the distance increases, but this is not always true. According to Shankar [2001], RSSI is inversely proportional to the square of the distance. To obtain the same amount of RSSI increase, a larger transmission power increase is needed at a longer distance. However, in reality, this rule doesn't always hold. For example, in Figures 2(a) and 2(c), the slopes of RSSI curves at a distance of 18 feet are bigger than those at a distance of 12 feet, which is caused by multipath reflection and scattering [Zhao and Govindan 2003]. Therefore, this measured correlation is a better reflection of the communication reality.

The shapes of RSSI/LQI curves based on the results from a grass field (Figures 2(a) and 2(b)), a parking lot (Figures 2(c) and 2(d)), and a corridor (Figures 2(e) and 2(f)) are significantly different from one another, even with the same distance and antenna direction between a pair of nodes. For example, with a transmission power level of 20 and a distance of 12 feet, the RSSI is −90dBm on a grass field (Figure 2(a)), while it is above −70dBm in a corridor (Figure 2(e)). Even though the curves for 12 feet on a grass field and on a parking lot are similar (Figures 2(a) and 2(c)), the 6-foot curves in these two environments are not quite the same (Figures 2(a) and 2(c)). These experimental results confirm that radio propagation among low-power sensor devices can be influenced largely by environment [Zhao and Govindan 2003; Zhou et al. 2004; Ganesan et al. 2002]. Moreover, RSSI/LQI with specified transmission power and distance varies in a very small range, and the degree of variations is related to the environment. According to the confidence intervals (97%) shown in Figure 2, RSSI readings are more stable than LQI. The confidence intervals of RSSI are not observable at most of the sampling points in Figures 2(a), 2(c), and 2(e).

2.2. Investigation of Temporal Impact

We also investigate the impact of time on the correlation between transmission power and link quality. Empirical results in this section suggest that this correlation changes slowly but noticeably over a long period of time. Therefore, online transmission power control is requisite to maintain the quality of communication over time.

A 72-hour outdoor experiment is conducted to demonstrate the variations of the radio communication quality over time. We place nine MICAz motes in a line with a 3-foot spacing. These motes are wrapped in Tupperware containers to protect against the weather. The Tupperware containers are placed in brushwood. They are about 0.5 feet high above the ground because the brushwood is very dense. During the experiment, each mote sends out a group of 20 packets at each transmission power level every hour. The transmission rate is 10 packets per second. All the other motes receive and record the average RSSI and the number of packets they received at each transmission power level. The transmissions of different motes are scheduled at different times to avoid collision.

In this experiment, data obtained from different pairs exhibit similar trends. Figure 3 presents our empirical data obtained from a pair of motes at a distance of 9 feet apart. Each curve represents the correlation between transmission power and RSSI at a specific time. The correlation between transmission power and RSSI every 8 hours is plotted in Figure 3(a). The shapes of these curves are different due to environmental dynamics. As a result, different transmission power levels are needed to reach the same link quality at different times. For example, to maintain an RSSI value at −89dBm, the transmission power level needs to be 11 at 0 AM on the first day, while at 4 PM on the second day the transmission power level needs to be 20. Figure 3(b) shows the hourly changes of the correlation. From Figure 3(b), we can see that the relation between transmission power and RSSI changes more gradually and continuously than that in

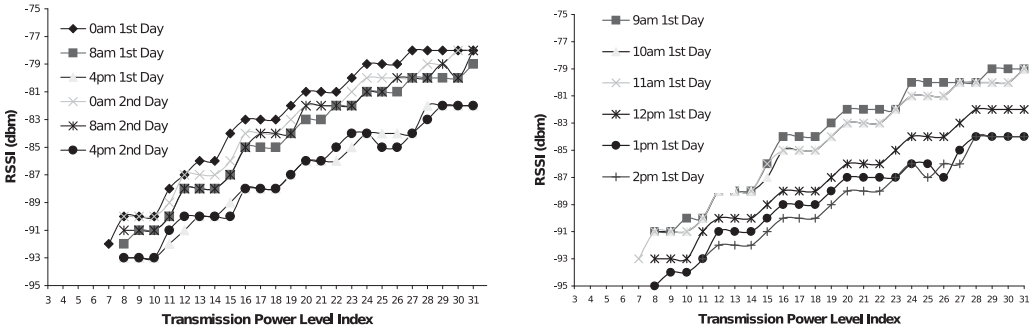

(a) Transmission Power *vs.* RSSI Sampling Every 8-hour

(b) Transmission Power *vs.* RSSI Sampling Every Hour

Fig. 3. Transmission power versus RSSI at different times.

Figure 3(a). For example, the maximum change in RSSI is 8dBm over an 8-hour period in Figure 3(a), while it is 3dBm over a 1-hour period in Figure 3(b).

These curves are approximately parallel, and the relationship between transmission power and RSSI varies differently at different times of day. For example, in Figure 3(a), the curve at 4 PM on the first day is much lower than the curve at 8 AM on the first day. The same variation happens on curves at 8 AM and 4 PM on the second day, but the degree of variation is different. All these results indicate that it is critical for transmission power control algorithms proposed for sensor networks to address the temporal dynamics of communication quality.

2.3. Dynamics of Transmission Power Control

To establish an effective transmission power control mechanism, we need to understand the dynamics between link qualities and RSSI/LQI values. In this section, we present empirical results that demonstrate the relation between the link quality and RSSI/LQI. The key observations, which serve as the basis of our work, are as follows:

—Both RSSI and LQI can be effectively used as binary link quality metrics for transmission power control.
—The link quality between a pair of motes is a detectable function of transmission power.

2.3.1. Link Quality Threshold. Wireless link quality refers to the radio channel communication performance between a pair of nodes. The PRR (packet reception ratio) is the most direct metric for link quality. However, the PRR value can only be obtained statistically over a long period of time. Our experiments indicate that both RSSI and LQI can be used effectively as binary link quality metrics for transmission power control.[1] We record the PRR and the average RSSI/LQI for every group of 100 packets from a grass field (Figures 4(a) and 4(d)), a parking lot (Figures 4(b) and 4(e)), and a corridor (Figures 4(c) and 4(f)). All experimental results show that both RSSI and LQI have a strong relationship with PRR. There is a clear threshold to achieve a nearly perfect PRR. However, these thresholds are slightly different in different environments. Take RSSI as an example: the 95% PRR threshold of RSSI is around −90dBm on the

[1]It is still controversial whether RSSI or LQI is a better indicator on link quality [Zhao and Govindan 2003; Reijers et al. 2004; Lal et al. 2003].

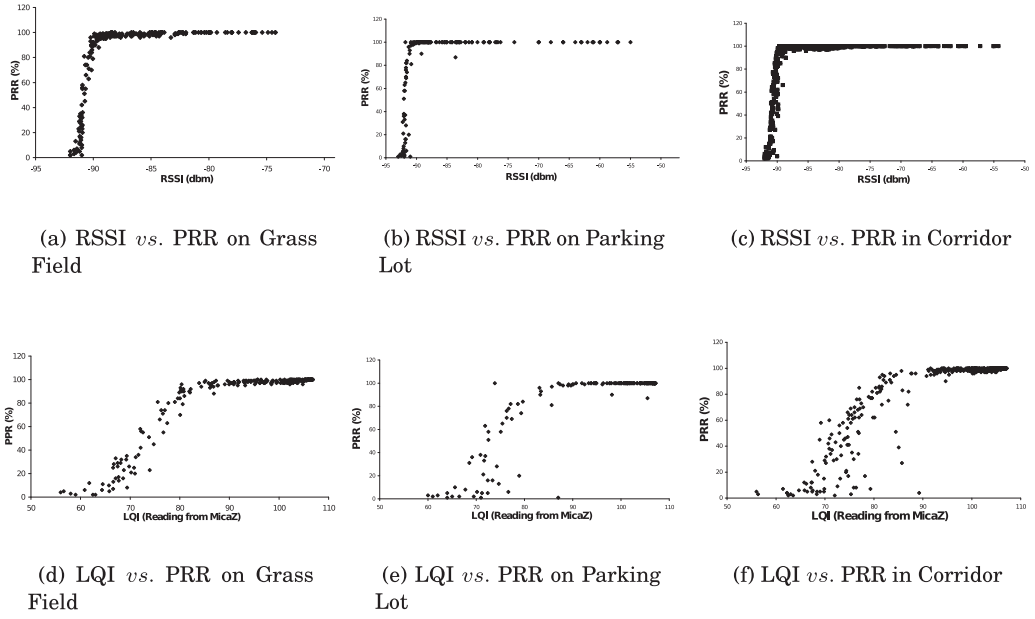

(a) RSSI *vs.* PRR on Grass Field

(b) RSSI *vs.* PRR on Parking Lot

(c) RSSI *vs.* PRR in Corridor

(d) LQI *vs.* PRR on Grass Field

(e) LQI *vs.* PRR on Parking Lot

(f) LQI *vs.* PRR in Corridor

Fig. 4. RSSI versus PRR in different environments.

grass field (Figure 4(a)), −91dBm on the parking lot (Figure 4(b)), and −89dBm in the corridor (Figure 4(c)).

2.3.2. Relations Between Transmission Power and RSSI/LQI. Radio irregularity results in radio signal strength variation in different directions, but the signal strength at any point within the radio transmission range has a detectable correlation with transmission power in a short time period.

In short-term experiments, the correlation between transmission power and RSSI/LQI for a pair of motes at a certain distance is generally monotonic and continuous. From Figure 2, the overall trend of RSSI increases linearly when the transmission power increases.

However, RSSI/LQI fluctuates in a small range at any fixed transmission power level. So, the correlation between transmission power and RSSI/LQI is not deterministic. For example, Figure 5 shows the RSSI upper bound and lower bound of 100 received packets at each transmission power level when we place two motes 6 feet apart on a grass field. This result confirms the observation from previous studies [Zhao and Govindan 2003; Zhou et al. 2004; Ganesan et al. 2002].

There are mainly three reasons for the fluctuation in the RSSI and LQI curves. First, fading [Shankar 2001] causes signal strength variation at any specific distance. Second, the background noise impairs the channel quality seriously when the radio signal is not significantly stronger than the noise signal. Third, the radio hardware doesn't provide strictly stable functionality [ChipconCC2420 2005].

Since the variation is small, this relation can be approximated by a linear curve. The correlation between RSSI and transmission power is approximately linear, and the correlation between LQI and transmission power is also approximately linear in a range. From the confidence intervals in Figure 2, we can see that RSSI and LQI are both relatively stable when these values are not small. All the points with confidence intervals bigger than 1 correspond to low link quality points in Figure 4, and the RSSI/LQI values that have the most fluctuations are below the good link quality

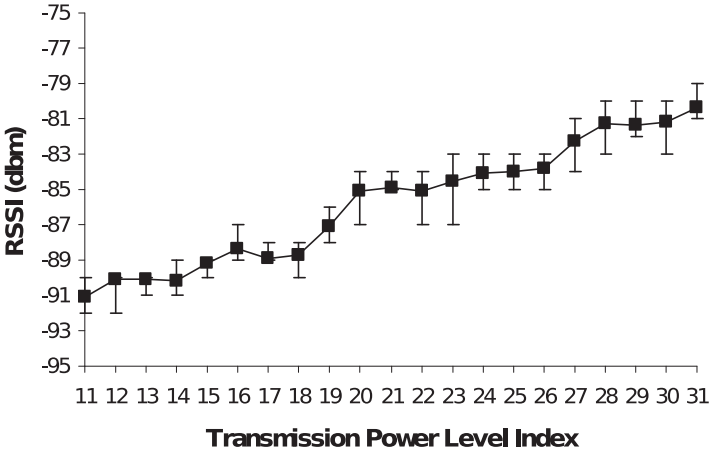

Fig. 5. Transmission power versus RSSI.

thresholds. Since we are only interested in RSSI/LQI samplings that are above or equal to the good link quality threshold, it is feasible to use a linear curve to approximate this correlation. This linear curve is built based on samples of RSSI/LQI. This curve roughly represents the in situ correlation between RSSI/LQI and transmission power.

This in situ correlation between transmission power and RSSI/LQI is largely influenced by environments, and this correlation changes over time. Both the shape and the degree of variation depend on the environment. This correlation also dynamically fluctuates when the surrounding environmental conditions change. The fluctuation is continuous, and the changing speed depends on many factors, among which the degree of environmental variation is one of the main factors.

3. DESIGN OF ATPC

Guided by the observations obtained from empirical experiments, in this section, we propose our Adaptive Transmission Power Control (ATPC) design. The objectives of ATPC are (1) to make every node in a sensor network find the minimum transmission power levels that can provide good link qualities for its neighboring nodes, to address the spatial impact, and (2) to dynamically change the pairwise transmission power level over time, to address the temporal impact. Through ATPC, we can maintain good link qualities between pairs of nodes with the in situ transmission power control.

Figure 6 shows the main idea of ATPC: a neighbor table is maintained at each node and a feedback closed loop for transmission power control runs between each pair of nodes. The neighbor table contains the proper transmission power levels that this node should use for its neighboring nodes and the parameters for the linear predictive models of transmission power control. The proper transmission power level is defined here as the minimum transmission power level that supports a good link quality between a pair of nodes. The linear transmission power predictive model is used to describe the in situ relation between the transmission powers and link qualities. Our empirical data indicate that this in situ relation is not strictly linear. Therefore, we cannot use this model to calculate the transmission power directly. Our solution is to apply feedback control theory to form a closed loop to gradually adjust the transmission power. It is known that feedback control allows a linear model to converge within the region when a nonlinear system can be approximated by a linear model, so we can safely design a small-signal linear control for our system, even if our linear model is just a rough approximation of reality.

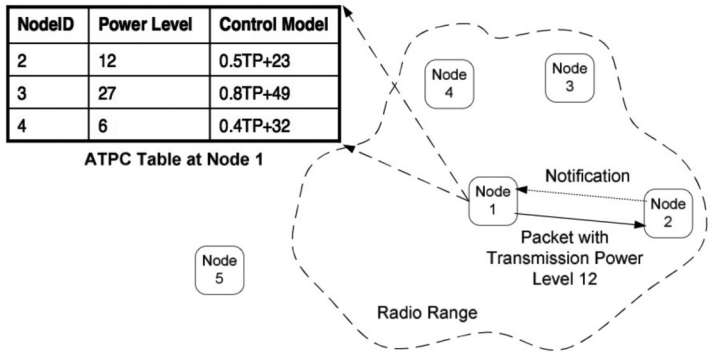

Fig. 6. Overview of the pairwise ATPC design.

3.1. Predictive Model for Transmission Power Control

The design objective is to establish models that reflect the correlation of the transmission power and the link quality between the senders and the receivers. Based on our empirical study and analysis in Section 2, we formulate a predictive model to characterize the relation between transmission power and link quality. Since no single model can capture precisely the per-network or even per-node behavior, we shall establish pairwise models, reflecting the in situ impact on individual links. Based on these models, we can predict the proper transmission power level that leads to the link quality threshold.

The idea of this predictive model is to use a function to approximate the distribution of RSSIs at different transmission power levels and to adapt to environmental changes by modifying the function over time. This function is constructed from sample pairs of the transmission power levels and RSSIs via a curve-fitting approach. To obtain these samples, every node broadcasts a group of beacons at different transmission power levels, and its neighbors record the RSSI of each beacon that they can hear and return those values.

We formulate this predictive model in the following way. Technically, this model uses a vector TP and a matrix R. $TP = \{tp_1, tp_2, \ldots, tp_N\}$. TP is the vector containing different transmission power levels that this mote uses to send out beacons. $|TP| = N$. N, the number of different transmission power levels, is subject to the accuracy requirement for applications. Ideally the more sampling data we have, the more accurate this model could be. Matrix R consists of a set of RSSI vectors R_i, one for each neighbor ($R = \{R_1, R_2, \ldots, R_n\}^T$). $R_i = \{r_i^1, r_i^2, \ldots, r_i^N\}$ is the RSSI vector for the neighbor i, in which r_i^j is an RSSI value measured at node i corresponding to the beacon sent by transmission power level tp_j. We use a linear function (Equation (1)) to characterize the relationship between transmission power and RSSI on a pairwise basis:

$$r_i(tp_j) = a_i \cdot tp_j + b_i. \tag{1}$$

We adopt a least square approximation, which requires little computation overhead and can be easily applied in sensor devices. Based on the vectors of samples, the coefficients a_i and b_i of Equation (1) are determined through this least square approximation method by minimizing S^2:

$$\sum \left(r_i(tp_j) - r_i^j\right)^2 = S^2. \tag{2}$$

Accordingly, the estimated value of a_i and b_i can be obtained in Equation (3):

$$\begin{bmatrix} \hat{a}_i \\ \hat{b}_i \end{bmatrix} = \frac{1}{N\sum_{j=1}^{N}(tp_j)^2 - \left(\sum_{j=1}^{N} tp_j\right)^2} \times \begin{bmatrix} \sum_{j=1}^{N} r_i^j \sum_{j=1}^{N}(tp_j)^2 - \sum_{j=1}^{N} tp_j \sum_{j=1}^{N} tp_j \cdot r_i^j \\ N\sum_{j=1}^{N} tp_j \cdot r_i^j - \sum_{j=1}^{N} tp_j \sum_{j=1}^{N} r_i^j \end{bmatrix}, \tag{3}$$

where i is the neighboring node's ID and j is the number of transmissions attempted. Using $\hat{a}_i$ and $\hat{b}_i$ together with a link quality threshold $RSSI_{LQ}$ identified based on experiments in Section 2.3, we can calculate the desired transmission power:

$$tp_j = \left[\frac{RSSI_{LQ} - \hat{b}_i}{\hat{a}_i}\right] \in TP,$$

where $[\cdot]$ means the function that rounds the inside value to the nearest integer in the set TP.

Note that Equation (3) only establishes an initial model. We need to update this model continuously while the environment changes over time in a running system. Basically, the values of a_i and b_i are functions of time. These functions allow us to use the latest samples to adjust our curve model dynamically. Based on our experimental results in Section 2, a_i, the slope of a curve, changes slightly in our 3-day experiment, while b_i changes noticeably over time. We assume the real model of the linear function for the relationship between transmission power and RSSI on a pairwise basis at time t is

$$r_i(tp(t)) = a_i \cdot tp(t) + b_i(t). \tag{4}$$

Therefore, once the predictive model of ATPC is built, a_i does not change any longer. $b_i(t)$ is calculated by the latest transmission power and RSSI pairs from the following feedback-based equation:

$$\begin{aligned} \Delta\hat{b}_i(t) &= \hat{b}_i(t) - \hat{b}_i(t+1) \\ &= \frac{\sum_{k=1}^{K}[RSSI_{LQ} - r_{i,k}(t-1)]}{K} \\ &= RSSI_{LQ} - r_i(t-1), \end{aligned} \tag{5}$$

where $r_i(t-1)$ is the average value of K readings denoted by

$$r_i(t-1) = \frac{1}{K}\sum_{k=1}^{K} r_{i,k}(t-1). \tag{6}$$

Here, $r_{i,k}(t-1), k = 1, \ldots, K$ is one reading of the RSSI value of the neighboring node i during time period $t-1$, and K is the number of feedback responses received from this neighboring node at time period $t-1$. Thus, we deduct the error (Equation (5)) from the previous estimation and get a new estimation of $b_i(t)$ as

$$\hat{b}_i(t) = \hat{b}_i(t-1) - \Delta\hat{b}_i(t). \tag{7}$$

The transmission power at time t is then adjusted given the adapted $\hat{b}_i(t)$ as

$$tp(t) = \left[\frac{RSSI_{LQ} - \hat{b}_i(t)}{a_i}\right]. \tag{8}$$

Although the link quality varies significantly over a long period of time, it changes gradually and continuously at a slow rate. Our experiments indicate that one packet

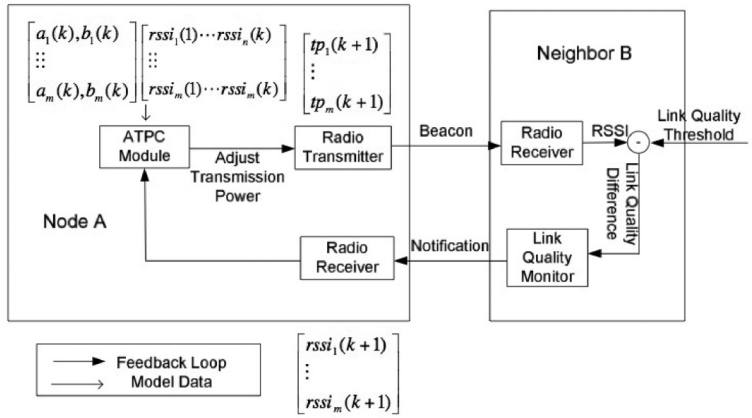

Fig. 7. Feedback closed loop overview for ATPC.

per hour between a pair is enough to maintain the freshness of the model in a natural environment. If the network has a reasonable amount of traffic, such as several packets per hour, nodes can use these packets to measure link quality change and piggyback RSSI readings. In this way, these models are refreshed with little overhead.

3.2. Analysis of ATPC Model

We use the average feedback value of RSSI to re-estimate $\hat{b}_i(t)$ and adjust the transmission power $tp(t)$ according to the desired RSSI threshold $RSSI_{LQ}$ at every time step t. In this subsection, we analyze conditions that the RSSI value will fall into the desired range when we apply the $tp(t)$ value computed by the ATPC model in this article.

We make the following assumptions in this subsection:

(1) We have the exact value of $RSSI_{LQ}$ (middle of the range of the upper bound $RSSI_H$ and lower bound $RSSI_L$ of RSSI value) set for ATPC model.
(2) The measurement of $r_{i,k}(t-1), k = 1, \ldots, K$ is accurate; that is, the RSSI value calculated from the real model equals the measured average value. It means

$$r_i(t-1) = r_i(tp(t-1)),$$

where $r_i(tp(t-1))$ represents the true RSSI value after we sent $tp(t-1)$ at time $t-1$.

3.2.1. When the Estimated $\hat{a}_i$ Is Equal to a_i. When the estimated slope $\hat{a}_i$ of Equation (4) equals the true value of a_i (from the experiment figures we know that $a_i > 0$), that is, $\hat{a}_i = a_i > 0$, the estimated model of Equation (4) only has a time-varying parameter $\hat{b}_i(t)$ to be adjusted:

$$\hat{r}_i(tp(t)) = a_i \cdot tp(t) + \hat{b}_i(t). \tag{9}$$

Here, $\hat{r}_i(tp(t))$ is the RSSI we calculate based on the newly estimated $\hat{b}_i(t)$ value at time t, given measurements of $r_i(t-1)$.

Assume we have received $r_i(tp(t)) = r_i(t)$, and $r_i(tp(t))$ is not in the desired range. To study the difference between $r_i(tp(t+1))$ and $r_i(tp(t))$, we plug Equation (8) of $tp(t)$ into

the model described in Equation (4) and get

$$\begin{aligned} & r_i(tp(t+1)) - r_i(tp(t)) \\ &= a_i \cdot tp(t+1) + b_i(t+1) - (a_i \cdot tp(t) + b_i(t)) \\ &= a_i \cdot \left(\left[\frac{RSSI_{LQ} - \hat{b}_i(t+1)}{a_i} \right] - \left[\frac{RSSI_{LQ} - \hat{b}_i(t)}{a_i} \right] \right) + b_i(t+1) - b_i(t). \end{aligned}$$

Here $tp(t)$ is an integer, such that

$$\frac{RSSI_{LQ} - \hat{b}_i(t)}{a_i} - 1 \leq tp(t) = \left[\frac{RSSI_{LQ} - \hat{b}_i(t)}{a_i} \right] \leq \frac{RSSI_{LQ} - \hat{b}_i(t)}{a_i} + 1.$$

Thus, $r_i(tp(t+1)) - r_i(tp(t))$ satisfies

$$\begin{aligned} & a_i \frac{\hat{b}_i(t) - \hat{b}_i(t+1)}{a_i} + b_i(t+1) - b_i(t) - 2a_i \\ &\leq r_i(tp(t+1)) - r_i(tp(t)) \\ &\leq a_i \frac{\hat{b}_i(t) - \hat{b}_i(t+1)}{a_i} + b_i(t+1) - b_i(t) + 2a_i. \end{aligned}$$

By Equation (5), the previous inequality is equivalent to

$$\begin{aligned} & RSSI_{LQ} - r_i(t) + b_i(t+1) - b_i(t) - 2a_i \\ &\leq r_i(tp(t+1)) - r_i(tp(t)) \\ &\leq RSSI_{LQ} - r_i(t) + b_i(t+1) - b_i(t) + 2a_i. \end{aligned}$$

To get a more accurate range of $r_i(tp(t+1)) - r_i(tp(t))$, we define ΔI_t to measure how much the integer approximation of $tp\,(t)$ differs from the original value of $\frac{RSSI_{LQ} - \hat{b}_i(t+1)}{a_i}$ as

$$\begin{aligned} \Delta I_t &= \left[\frac{RSSI_{LQ} - \hat{b}_i(t)}{a_i} \right] - \frac{RSSI_{LQ} - \hat{b}_i(t)}{a_i}, \\ \Delta I_{t+1} &= \left[\frac{RSSI_{LQ} - \hat{b}_i(t+1)}{a_i} \right] - \frac{RSSI_{LQ} - \hat{b}_i(t+1)}{a_i}, \end{aligned}$$

where $|\Delta I_t| < 1, t = 1, 2, \ldots,$ and then

$$r_i(tp(t+1)) - r_i(tp(t)) = RSSI_{LQ} - r_i(t) + a_i(\Delta I_{t+1} - \Delta I_t) + b_i(t+1) - b_i(t).$$

The value of $r_i(tp(t+1))$ satisfies

$$r_i(tp(t+1)) = RSSI_{LQ} + a_i(\Delta I_{t+1} - \Delta I_t) + b_i(t+1) - b_i(t). \tag{10}$$

We then derive conditions that $r_i(tp(t+1))$ falls in different ranges based on Equation (10).

The necessary and sufficient condition for $RSSI_L \leq r_i(tp\,(t+1)) \leq RSSI_H$ is

$$\begin{aligned} RSSI_L - RSSI_{LQ} - a_i(\Delta I_{t+1} - \Delta I_t) &\leq b_i(t+1) - b_i(t) \\ &\leq RSSI_H - RSSI_{LQ} - a_i(\Delta I_{t+1} - \Delta I_t). \end{aligned} \tag{11}$$

The necessary and sufficient condition for $r_i(tp\,(t+1)) < RSSI_L$ is

$$b_i(t+1) - b_i(t) < RSSI_L - RSSI_{LQ} - a_i(\Delta I_{t+1} - \Delta I_t).$$

The necessary and sufficient condition for $r_i(tp(t+1)) > RSSI_H$ is

$$b_i(t+1) - b_i(t) > RSSI_H - RSSI_{LQ} - a_i(\Delta I_{t+1} - \Delta I_t).$$

A special case when $r_i(tp(t+1))$ will always fall in the desired range: Since $|\Delta I_t| < 1, |\Delta I_{t+1}| < 1$, $\Delta I_{t+1} - \Delta I_t$ is bounded in

$$|\Delta I_{t+1} - \Delta I_t| < 2.$$

When $RSSI_H - RSSI_L > 4a_i (a_i > 0)$, the following inequalities always hold:

$$RSSI_L - RSSI_{LQ} - a_i(\Delta I_{t+1} - \Delta I_t) < 0,$$
$$RSSI_H - RSSI_{LQ} - a_i(\Delta I_{t+1} - \Delta I_t) > 0.$$

When $b_i(t) = b_i(t+1)$ is satisfied (i.e., the true parameter b_i does not change with time), we always have $r_i(tp(t+1)) \in [RSSI_L, RSSI_H]$, because the following inequality is true:

$$RSSI_L - RSSI_{LQ} - a_i(\Delta I_{t+1} - \Delta I_t) \leq 0 \leq RSSI_H - RSSI_{LQ} - a_i(\Delta I_{t+1} - \Delta I_t).$$

This is a special case when the assumptions in Equations (1) and (2) hold, and $b_i(t)$ stays static during time t and $t+1$; we directly get a desired RSSI value by the ATPC method introduced in this article.

Conclusion: We summarize the previous process to reach the following conclusion: given the function of the relation between transmission power and RSSI at time $t, t+1$ as in Equation (4), and the condition that the estimation of the slope is accurate, that is, $\hat{a}_i = a_i$, the RSSI value will be in the desired range ($r_i(t+1) \in [RSSI_L, RSSI_H]$) if and only if the difference between $b_i(t), b_i(t+1)$ satisfies Equation (11).

3.2.2. When the Estimation of a_i Has an Error Δa_i. In the previous model analysis section, we assume that the real a_i does not change with time, that is, $a = a_i(1) = a_i(2) = a_i(3) = \ldots$, and we have an accurate estimation of a_i, that is, $\hat{a}_i = a_i > 0$. In practice, this may not be the case, and it is possible that the real $a_i(t)$ slightly changes with time t or the estimated $\hat{a}_i$ we use in Equation (9) is inaccurate. In either case, the estimation error is bounded, and we show the complete conditions for $r_i(tp(t+1))$ to be regulated inside $[RSSI_L, RSSI_H]$, considering errors of $\hat{a}_i$ and value changes of $b_i(t)$.

We assume the real $a_i(t)$ in Equation (4) is the estimated $\hat{a}_i$ in Equation (9) plus some bounded error. Define the estimation error $\Delta a_i(t)$ as

$$a_i(t) = \hat{a}_i + \Delta a_i(t),\ \ \Delta a_i(t) \in \mathbb{R},\ \ |\Delta a_i(t)| < \epsilon_i,\ \ t = 1, 2, \ldots. \tag{12}$$

In the following discussion, we show how $\Delta a_i(t)$ will affect the results when we adjust the transmission power according to an inaccurate $\hat{a}_i$.

Considering inaccurate $\hat{a}_i$, we define the transmission power according to measured average $r_i(t)$, estimated $\hat{b}_i(t), \hat{a}_i$ as

$$tp(t) = \left\lceil \frac{RSSI_{LQ} - \hat{b}_i(t)}{\hat{a}_i} \right\rceil. \tag{13}$$

Assume the integer approximation has a tail measured by

$$\Delta I'_t = \left\lceil \frac{RSSI_{LQ} - \hat{b}_i(t)}{\hat{a}_i} \right\rceil - \frac{RSSI_{LQ} - \hat{b}_i(t)}{\hat{a}_i}. \tag{14}$$

To show the conditions for $r(tp(t+1)) \in [RSSI_L, RSSI_H]$ when $\hat{a}_i \neq a_i(t)$ or $\hat{a}_i \neq a_i(t+1)$ or $a_i(t) \neq a_i(t+1)$, we derive the equation of $r(tp(t+1))$ similar to the analysis process

for time-invariant $\hat{a}_i = a_i$:

$$
\begin{aligned}
& r_i(tp(t+1)) - r_i(tp(t)) \\
&\quad = a_i(t+1)\cdot tp(t+1) + b_i(t+1) - (a_i(t)\cdot tp(t) + b_i(t)) \\
&\quad = a_i(t+1)\left(\frac{RSSI_{LQ} - \hat{b}_i(t+1)}{\hat{a}_i} + \Delta I'_{t+1}\right) - a_i(t)\left(\frac{RSSI_{LQ} - \hat{b}_i(t)}{\hat{a}_i} + \Delta I'_t\right) \\
&\qquad + b_i(t+1) - b_i(t) \\
&\quad = (2RSSI_{LQ} - r_i(t) - \hat{b}_i(t))\left(1 + \frac{\Delta a_i(t+1)}{\hat{a}_i}\right) - (RSSI_{LQ} - \hat{b}_i(t))\left(1 + \frac{\Delta a_i(t)}{\hat{a}_i}\right) \\
&\qquad + (\hat{a}_i + \Delta a_i(t+1))\Delta I'_{t+1} - (\hat{a}_i + \Delta a_i(t))\Delta I'_t + b_i(t+1) - b_i(t) \\
&\quad = RSSI_{LQ}\left(1 + \frac{2\Delta a_i(t+1) - \Delta a_i(t)}{\hat{a}_i}\right) - (\hat{a}_i + \Delta a_i(t))\Delta I'_t \\
&\qquad + \hat{b}_i(t)\frac{\Delta a_i(t) - \Delta a_i(t+1)}{\hat{a}_i} + (\hat{a}_i + \Delta a_i(t+1))\Delta I'_{t+1} \\
&\qquad - r_i(t)\left(1 + \frac{\Delta a_i(t+1)}{\hat{a}_i}\right) + b_i(t+1) - b_i(t).
\end{aligned}
$$

Assume the measured RSSI is a true value (or the error can be neglected), that is, $r_i(t) = r_i(tp(t))$; then

$$
\begin{aligned}
& r_i(tp(t+1)) \\
&\quad = RSSI_{LQ}\left(1 + \frac{2\Delta a_i(t+1) - \Delta a_i(t)}{\hat{a}_i}\right) - r_i(t)\frac{\Delta a_i(t+1)}{\hat{a}_i} \\
&\qquad + \hat{b}_i(t)\frac{\Delta a_i(t) - \Delta a_i(t+1)}{\hat{a}_i} + (\hat{a}_i + \Delta a_i(t+1))\Delta I'_{t+1} - (\hat{a}_i + \Delta a_i(t))\Delta I'_t + b_i(t+1) - b_i(t).
\end{aligned}
$$

Thus, conditions for $r_i(tp(t+1))$ to fall in different intervals are described as follows:
Condition for $RSSI_L \le r_i(tp(t+1)) \le RSSI_H$:

$$
\begin{aligned}
& RSSI_L - RSSI_{LQ}\left(1 + \frac{2\Delta a_i(t+1) - \Delta a_i(t)}{\hat{a}_i}\right) + r_i(t)\frac{\Delta a_i(t+1)}{\hat{a}_i(j)} \\
&\qquad + \hat{b}_i(t)\frac{\Delta a_i(t) - \Delta a_i(t+1)}{\hat{a}_i} + (\hat{a}_i + \Delta a_i(t+1))\Delta I'_{t+1} - (\hat{a}_i + \Delta a_i(t))\Delta I'_t \\
&\quad \le b_i(j+1) - b_i(j) \\
&\quad \le RSSI_H - RSSI_{LQ}\left(1 + \frac{2\Delta a_i(t+1) - \Delta a_i(t)}{\hat{a}_i}\right) + r_i(t)\frac{\Delta a_i(t+1)}{\hat{a}_i(j)} \\
&\qquad + \hat{b}_i(t)\frac{\Delta a_i(t) - \Delta a_i(t+1)}{\hat{a}_i} + (\hat{a}_i + \Delta a_i(t+1))\Delta I'_{t+1} - (\hat{a}_i + \Delta a_i(t))\Delta I'_t
\end{aligned}
\tag{15}
$$

Compare the above inequality with (11), the last two items with $\Delta I'_{t+1}$ and $\Delta I'_t$ are related to $\Delta a_i(t+1)$ and $\Delta a_i(t)$, respectively. When $\Delta a_i(t) \approx 0$ and $\Delta a_i(t+1) \approx 0$, or the estimation error of $\hat{a}_i$ is negligible, inequality (15) reduces to the form of (11).

Similarly, conditions for $r_i(tp(t+1))$ outside the range $[RSSI_L, RSSI_H]$ are as follows:
Condition for $r_i(tp(t+1)) < RSSI_L$:

$$\begin{aligned} & b_i(t+1) - b_i(t) \\ & < RSSI_L - RSSI_{LQ}\left(1 + \frac{2\Delta a_i(t+1) - \Delta a_i(t)}{\hat{a}_i}\right) + r_i(t)\frac{\Delta a_i(t+1)}{\hat{a}_i(j)} \\ & \quad + \hat{b}_i(t)\frac{\Delta a_i(t) - \Delta a_i(t+1)}{\hat{a}_i} + (\hat{a}_i + \Delta a_i(t+1))\Delta I'_{t+1} - (\hat{a}_i + \Delta a_i(t))\Delta I'_t \end{aligned}$$

Condition for $r_i(tp(t+1)) > RSSI_H$:

$$\begin{aligned} & b_i(t+1) - b_i(t) \\ & > RSSI_H - RSSI_{LQ}\left(1 + \frac{2\Delta a_i(t+1) - \Delta a_i(t)}{\hat{a}_i}\right) + r_i(t)\frac{\Delta a_i(t+1)}{\hat{a}_i(j)} \\ & \quad + \hat{b}_i(t)\frac{\Delta a_i(t) - \Delta a_i(t+1)}{\hat{a}_i} + (\hat{a}_i + \Delta a_i(t+1))\Delta I'_{t+1} - (\hat{a}_i + \Delta a_i(t))\Delta I'_t \end{aligned}$$

Conclusion: Considering both the estimation error and value change of parameters $a_i(t)$, $b_i(t)$ in Equation (9), we show a similar inequality form of conditions for $r_i(tp(t+1))$ to be in the desired range. When the estimation error of $a_i(t)$ is insignificant, the conditions reduce to the same with those in Section 3.2.1.

The conditions for $r_i(tp(t+1))$ to fall in $[RSSI_L, RSS_H]$ are related to the difference between the true values of $b_i(t+1)$ and $b_i(t)$. The adjustment process requires that $b_i(t+1) - b_i(t)$ is in a specific range to terminate the transmission power adjustment. When the RSSI feedback value keeps oscillating outside the desired range after many steps, one possible reason is that the difference between $b_i(t+1)$ and $b_i(t)$ is outside the corresponding range. If we increase the sampling rate under this case, the range width of $b_i(t+1) - b_i(t)$ is expected to reduce, since the true parameters of Equation (4) are expected to vary in a smaller way in a shorter time. Hence, we have a better chance to regulate the signal strength inside the desired range in fewer following steps by increasing the sampling rate.

3.3. Adaptive Design

3.3.1. Adaptive Sampling. The adaptive transmission power controller can use both data and control packets to obtain link quality samples; RSSI feedbacks of these packets from neighboring nodes are sent back to the controller to adjust the transmission power level and update the ATPC control model during runtime. Regardless of feedback packet loss, the ATPC controller obtains a sample on each link quality when the sender node transmits a packet and the receiver node receives it.

The traditional control designs [Jung and Vaidya 2002; He et al. 2003] typically require a fixed sampling rate so that the control loop can capture the changes of the measured signal and take adjustments. This sampling rate poses a tradeoff on control performance and cost. A high sampling rate provides prompt information on the link quality, but it also uses more bandwidth and energy to transmit these packets. A low sampling rate reduces the control cost in terms of bandwidth and energy but can cause the power control to converge slowly, even causing temporary packet loss. A good sampling rate is very important for control design to achieve desired stability and control accuracy.

We propose an adaptive sampling approach to find a good tradeoff between control performance and cost. The adaptive sampling design achieves both fast reactions to link dynamics and low energy cost. The basic idea is to change the sampling rate according to the dynamics of link quality. When the link quality varies quickly and

data packets go along this link, nodes need to sample link quality at a high rate for agile reaction to link quality changes. On the other hand, nodes sample link quality at a low rate when link quality does not change significantly or few data packets go along this link to save energy.

The adaptive transmission power control changes the sampling rate in the following four events:

—If either one of the following two conditions happen, a node decreases the sampling rate by a factor of p: (1) the received signal strength of the incoming packet stays within the specified range of good link quality, or (2) no data packets are transmitted along this link in the last sampling cycle.
—A node increases the sampling rate by a factor of q if received signal strength of the incoming packet changes significantly outside the specified range of good link quality by a threshold s.
—A node transmits an on-demand sampling packet if it receives a packet request for sampling from a neighbor node. A neighbor requests for sampling if it does not hear from the sender for a long period l, to maintain link connectivity in case data packets and regular sampling packets on this link get lost.
—Data packets can serve as the sampling packets and feedback packets. If data packets are transmitted in a sampling period, nodes change the sampling rate in the following two conditions: (1) if the RSSI samples stay within the specified range of good link quality, only the last data packet in this period serves as the sampling packet, and (2) if some RSSI samples do not stay within the specified range of good link quality, these packets serve as the sampling packets.

In a network with stable link qualities, both the second and third conditions rarely happen. Therefore, the sampling rate decreases exponentially, up to a constant threshold R_{high}. When the link quality varies significantly, affected nodes reset their sampling rate to R_{low}. So the power control can converge quickley without losing packets.

3.3.2. Adaptive Link Quality Threshold. The set point value in the transmission power control is critical for our power control design to achieve reliable link quality. This set point represents the minimum receiving signal strength of packets that allows them to be received reliably. The underlying model of this design is the SNR model [Tse and Viswanath 2005; Sarkar et al. 2007]. According to the SNR model, if the signal power (represented by RSSI)–to–background noise power ratio is larger than a fixed value, the noise cannot corrupt the signal. Therefore, if the background noise level does not change, the RSSI reading can determine if the packets can be received successfully.

Existing topology control works usually assume a fixed link quality threshold in all environments. However, this simplified assumption does not hold in real systems. The background noise level may change in different locations and over time. Adjusting the RSSI threshold based on the background noise level is critical for our power control design. If we use a high RSSI threshold as the set point, the link would be reliable but the energy saving is limited. In order to save energy, we should use a low RSSI threshold as the set point, but it can cause packet loss where the background noise level is high.

To find an accurate RSSI threshold, we have conducted extensive experiments in different locations and environments. Our experimental results show that the RSSI threshold has different values in different environments, as shown in Section 2.3.1: the 95% PRR threshold of RSSI is around −90dBm on the grass field (Figure 4(a)), −91dBm on the parking lot (Figure 4(b)), and −89dBm in the corridor (Figure 4(c)). These empirical values serve as the basis for our selection of the set point in real deployment.

3.4. Reliable Unicast, Multicast, and Broadcast

In wireless sensor networks, unicast, multicast, and broadcast are three main communication services to transfer information from one node to other nodes. By integrating ATPC with these main communication paradigms at the MAC layer, we achieve reliable unicast, multicast, and broadcast. For each packet transmission, the power control integration allows us to use the transmission power (if existing) that can achieve reliable packet delivery. The existing MAC layer services need to be modified slightly. Here we propose our designs for power-controlled unicast, multicast, and broadcast.

Unicast at the MAC layer typically transmits a packet with default transmission power. With ATPC, at the MAC layer, every unicast procedure needs to find the corresponding transmission power level in the ATPC neighbor table given the neighbor id in the packet, and then set the transmission power level before the original procedure. The power level provided by the ATPC table also indicates whether this neighbor is within the node's reliable communication range. For example, if the transmission power level is less than the maximum, packets transmitted to this neighbor will be reliably received.

Multicast and broadcast with power control are also important, since many routing protocols, such as the Geographic Forwarding (GF) algorithm, rely on reliable links to forward packets to next-hop neighbors. ATPC provides the reliable link list that can be naturally used by these routing protocols. Therefore, we design MAC layer multicast and broadcast with ATPC.

Since broadcast is a special case of multicast, here we use multicast to illustrate our design. When a multicast transmission is processed to send a packet to a subset of neighbors, it needs to find the maximal transmission power level of the transmission power levels for these neighbors in the ATPC table, and then set this power level for the multicast transmission. Every neighbor in this multicast subset who receive this packet will transmit a feedback to the sender with its RSSI as feedback. The power controller at the sender makes a model update only on the entries where the transmission power levels are obtained.

In the following three conditions, the reliable neighbor set changes: dramatic link quality changes, a new node appears, and an original node disappears. ATPC automatically detects link quality variations over time and updates the reliable neighbor set, as well as nodes joining/leaving the network, since it has periodic beacons with maximum power level, which keeps all the topology information.

For other routing algorithm designs, such as opportunistic routing, ATPC is not suitable and nodes should use the maximum transmission power for each packet transmission.

3.5. Implementation of ATPC

The implementation of ATPC on sensor devices is presented in this subsection. We discuss mainly four aspects: (1) the two-phase design and the feedback closed loop for pairwise transmission power control, (2) the parameters that affect system performance, (3) the techniques that optimize system performance and reduce cost, and (4) the other issues.

ATPC has two phases, the initialization phase and the runtime tuning phase.

In the initialization phase, a mote computes a predictive model and chooses a proper transmission power level based on that model for each neighbor. Since wireless communication is broadcast in nature, all the neighbors can receive beacons and measure link qualities in parallel. Based on this property, every node broadcasts beacons with different transmission power levels in the initialization phase, and its neighbors measure RSSI/LQI values corresponding to these beacons and send these values back by a notification packet.

In the runtime tuning phase, a lightweight feedback mechanism is adopted to monitor the link quality change and tune the transmission power online. Figure 7 is an overview picture of the feedback mechanism in ATPC. To simplify the description, we show a pair of nodes. Each node has an ATPC module for transmission power control. This module adopts a predictive model described in the previous subsection for each neighbor. It also maintains a list of proper transmission power levels for neighbors of this mote. When node A has a packet to send to its neighbor B, it first adjusts the transmission power to the level indicated by its neighbor table in the ATPC module and then transmits the packet. When receiving this packet, the link quality monitor module at its neighbor B takes a measurement of the link quality. Based on the difference between the desired link quality and actual measurements, the link quality monitor module decides whether a notification packet is necessary. A notification packet is necessary when (1) the link quality falls below the desired level or (2) the link quality is good but the current signal energy is so high that it wastes the transmission energy. The notification packet contains the measured link quality difference. When node A receives a notification from its neighbor B, the ATPC module in node A uses the link quality difference as the input to the predictive model and calculates a new transmission power level for its neighbor B.

If achieving good link quality requires using the maximum transmission power level, ATPC adjusts the transmission power to the maximum level. If using the maximum transmission power level cannot achieve good link quality, this link is marked so that routing protocols, like those in Singh et al. [1998], Lin et al. [2009], Subbarao [1999], Gomez et al. [2003], Ganesan et al. [2001], Chipara et al. [2006], and Lin et al. [2008], can choose another route based on the neighbor table provided by ATPC. If all the routes cannot provide good link quality, the mote can do best-effort transmission to a neighbor with relative good link quality by using the maximum transmission power level.

There is a tradeoff between accuracy and cost when applying ATPC. The practical values of these parameters are obtained from analysis and empirical results. These important parameters include the link quality thresholds, the sampling rate of transmission power control, the number of sample packets in the initialization phase, and the small-signal adjustment of transmission power control, which is proportional to the link quality error. Choices of parameters are essential for obtaining good performance.

The link quality monitor can have any of the following three criteria to estimate link quality changes. The first one is the link quality reflected by the RSSI value, the second one is the LQI value if available, and the last one is the packet reception ratio as detected by sequence number monitoring. Our design is compatible with all these methods. Without loss of generality, we use both RSSI and PRR in our experiments. We note that the theory described in Section 3.1 provides good guidance in ideal conditions.

To monitor the link quality by referring to RSSI values, we set two link quality thresholds. LQ_{upper} is an upper threshold and LQ_{lower} is a lower threshold. As long as the RSSI value of the received packet lies within this range, the system is in the steady state. When a link is in the steady state, the receiver does not need to send a notification packet to the sender, and the sender does not adjust the transmission power. The range of $[LQ_{lower}, LQ_{upper}]$ is critical to energy savings and tuning accuracy. If the range of $[LQ_{lower}, LQ_{upper}]$ is too small, radio signal fading may result in the oscillation of transmission power. If the range of $[LQ_{lower}, LQ_{upper}]$ is too big, the transmission power control result may not be accurate enough, and the optimal power control will not be achieved. In our implementation, the value of LQ_{lower} is chosen to guarantee that the link quality does not drop below the tolerance level. With respect to LQ_{upper} in our design, its value is chosen to trade off the energy cost paid to transmit notifications and the energy saved to transmit data packets. This is a simple calculation for choosing LQ_{upper}, which compares the energy consumed by sending a control packet with the

energy saved for n data packets after tuning the transmission power. In our experiment, we use $n = 2$ for simplicity. Thus, energy savings are achieved when at least two data packets are transmitted using the tuned transmission power level, compared to the energy consumed by transmitting a notification packet.

A good feedback sampling rate is essential to maintain the link quality at a desired level while minimizing the control overhead. Two main factors influence the feedback sampling rate: link quality dynamics and network traffic. On one hand, the higher the link quality dynamics, the higher the sampling rate needed. Based on our empirical results in Figure 3, the maximum link quality variation per 8 hours is 8dBm, and the maximum link quality variation per hour is 3dBm. In order to keep the link quality error under 3dBm, a sampling rate of one packet per hour is necessary. On the other hand, the regular network traffic can be used for ATPC sampling purposes and considered as ATPC's input. When the network traffic is higher than this sampling rate, notification packets can be sent on demand. There is only a low number of notification packets needed, and the control overhead is minimized. Our running system evaluation demonstrates that this design is very efficient. On average, eight on-demand notification packets are sent per link per day to deal with the runtime link quality dynamics.

In applications with periodic multihop traffic, an overhearing approach can save the overhead of notification packets. Along the data transfer route, when a node is forwarding packets to its next hop, it can incorporate an extra byte to record the RSSI value of the previous hop transmission in the packet, and then the sender of the previous hop can overhear the corresponding RSSI, thus eliminating explicit notifications.

Another optimization technique is to use ATPC only on critical paths with heavy traffic, so ATPC can extend the system lifetime while supporting a high-quality end-to-end communication with little control overhead. For those links with a low traffic load, directly using a conservative transmission power level is a good tradeoff between communication quality and energy savings. This is because nodes do not need to periodically generate control packets to monitor link quality.

Based on our empirical results, the RSSI readings can be affected by stochastic environmental noise. For example, the RSSI with a certain beacon packet can be unexpectedly high or low, which is inconsistent with the monotonic relationship between transmission power and RSSI. Filtering such noise input can enhance the accuracy of ATPC's modeling. On the other hand, if some RSSI with a certain transmission power level falls in our desired link quality range, using the corresponding transmission power level directly also enhances ATPC's performance.

The code for ATPC mainly includes functions for linear approximation. The code size is 14,122 bytes in ROM. The data structures in ATPC mainly include a neighbor table, a vector TP, and a matrix R as described in Section 3.1. For a node with 20 neighbors, the data size is 2,167 bytes in RAM.

4. EXPERIMENTAL EVALUATION

ATPC is evaluated in outdoor environments. We first evaluate ATPC's predictive model described in Section 3.1 with a short-term experiment. We then describe a 72-hour experiment to compare ATPC against network-level uniform transmission power solutions and a node-level nonuniform transmission power solution. According to our empirical results, ATPC's advantages lie in three core aspects:

(1) ATPC maintains high communication quality over time in changing weather conditions. It has significantly better link qualities than using static transmission power in a long-term experiment, which confirms our observations in Section 2.2. Moreover, it maintains equivalent link qualities as using the maximum transmission power solution.

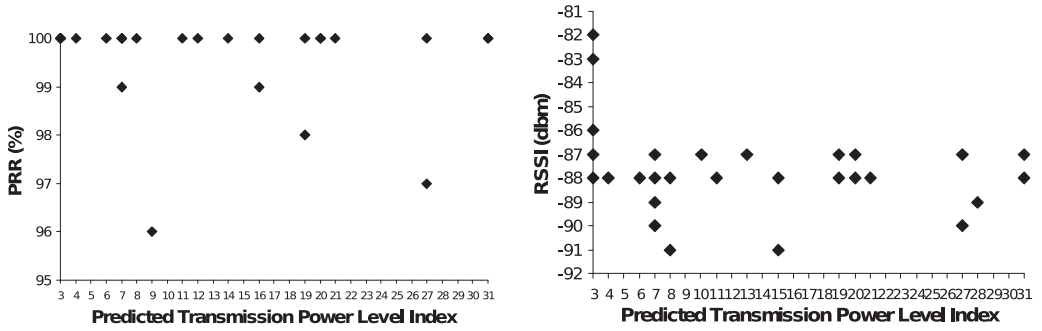

(a) Predicated Transmission Power Level *vs.* PRR

(b) Predicated Transmission Power Level *vs.* RSSI

Fig. 8. Prediction accuracy.

(2) ATPC achieves significant energy savings compared to other network-level transmission power solutions. ATPC only consumes 53.6% of the transmission energy of the maximum transmission power solution and 78.8% of the transmission energy of the network-level transmission power solution.
(3) ATPC accurately predicts the proper transmission power level and adjusts the transmission power level in time to meet environmental changes, adapting to spatial and temporal factors.

4.1. Initialization Phase

In the initialization phase of ATPC, each mote broadcasts a group of beacons. Its neighbors record the RSSI and the corresponding transmission power level of each beacon that they can hear and then send them back to the beaconing node. Using these pairs of values as input for the ATPC module, the beaconing node builds the predictive models and computes the transmission power level for each of its neighbors.

To evaluate the accuracy of the initialization phase, an experiment is conducted in a parking lot with eight MICAz motes; it is repeated 5 times. These motes are put in a line 3 feet apart from adjacent nodes. Each mote runs ATPC's initialization phase in a different time slot, sending out eight beacons at a fixed rate using different transmission power levels. These transmission power levels are distributed uniformly in the transmission power range supported by the CC2420 radio chip. After the initialization phase of ATPC, each mote sends a group of 100 packets to its neighbors using predicted transmission power levels. Its neighbors record the average RSSI and PRR. The experimental results are shown in Figures 8(a) and 8(b). Every point in Figure 8(a) demonstrates a pair of the predicted transmission power level and the PRR when using that power level. In all these experiments, the average PRR is 99.0%. From Figure 8(a), we can see that all the RSSI readings are above or equal to −91dBm. The standard deviation of the RSSI is 2. According to Section 2.3.1, RSSIs that are above −91dBm mean good link quality in a parking lot. These results prove that the predictive model of ATPC works well. Moreover, in our long-term experiments, the predicted transmission power levels of all the nodes that were obtained in ATPC's initialization phase are in the desired range.

4.2. Runtime Performance

To evaluate the runtime performance, we compare ATPC against existing transmission power control algorithms: network-level uniform solutions and a node-level nonuniform

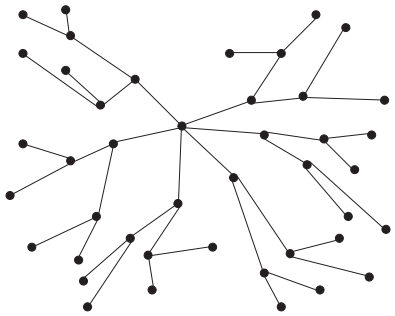

Fig. 9. Topology.

Fig. 10. Experimental site.

solution (Nonuniform). Two kinds of network-level transmission power levels are used: the max transmission power level (Max) and the minimum transmission power level over nodes in the network that allows them to reach their neighbors (Uniform). A 72-hour continuous experiment is conducted to evaluate the energy savings and communication quality of ATPC over time. The empirical data shows that ATPC achieves the best overall performance in terms of communication quality and energy consumption. The 3-hop end-to-end PRR of ATPC is constantly above 98% over 3 days, and ATPC greatly saves transmission power consumption compared to network-level uniform transmission power solutions.

4.2.1. Experiment Setup. A 72-hour experiment is conducted on a grass field with 43 MICAz motes. These motes are deployed according to a randomly generated topology. They form a spanning tree as shown in Figure 9. The root of the spanning tree is at the center of Figure 9. The deployed area is a 15-by-15-meter square. Figure 10 is a picture of the node deployment for one of our experiments on a grass field. All the motes are placed in Tupperware containers to protect against the weather. According to our experiments, these plastic boxes (nonconducting material) do not attenuate radio waves significantly.

There are 24 total leaf nodes in this spanning tree. These leaf nodes report data to the base node hourly. Each hour is evenly divided into 24 time slots, and different leaf nodes are assigned to different time slots. Transmissions of different motes are scheduled at different times to avoid collision. Each leaf node reports 32 packets to the base node at a transmission rate of 15 packets per minute in its time slot. These packets are divided into four groups, corresponding to different transmission power control solutions: ATPC, Max, Uniform, and Nonuniform. These four algorithms are evaluated in the same environment. The predicted transmission power level obtained in ATPC's initialization phase is used for Nonuniform, which satisfies the assumption that it is the minimum transmission power for each node to reach its neighbors. We use the maximum predicted transmission power level of all nodes obtained in ATPC's initialization phase for Uniform. This transmission power level is the minimum transmission power level over all nodes to reach their neighbors. Max, Uniform, and Nonuniform all use static transmission power. The statistical data about number of packets sent and received and the transmission power level used for each solution are recorded at each mote. In this experiment, for simplicity, each node considers its parent in the spanning tree as its neighbor. This experiment is deployed at 6 PM on March 19 and finished at 7 PM on March 22. There was a shower that lasted for 2 hours on the morning of March 21. Figure 11 shows the weather conditions of these days.

Date	March 19	March 20	March 21	March 22
High	56º F	54º F	41º F	49º F
Low	27º F	31º F	31º F	30º F
Precip.	0 inch	0 inch	0.05 inch	0 inch
Condition	Fair	Mostly Fair	Cloudy, Light Rain during 10am ~ 12am	Mostly Fair

Fig. 11. Weather conditions over 72 hours.

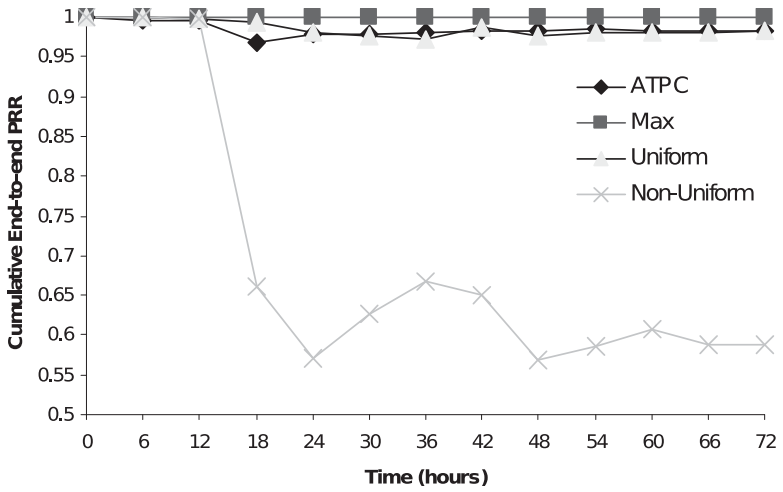

Fig. 12. E2E PRR.

4.2.2. Data Delivery Ratio. Figure 12 shows the cumulative end-to-end PRR over time. From this figure, we can see that Max achieves 100% end-to-end PRR all the time. As using the maximum transmission power makes the RSSI values at the receiver the highest of all solutions, it is robust to random environmental changes and noise.

ATPC and Uniform both achieve around 98% cumulative end-to-end PRR. ATPC has a little better performance than Uniform for 83% of the experimental time. However, the reasons for packet loss of these two solutions are quite different. For ATPC, half of these end-to-end links have 100% PRR. The other 12 links from leaves to the base node suffer from random packet loss from time to time. For Uniform, the packet loss mainly happens at two specific links. These links have the same predicted transmission power level as the uniform transmission power level. We pick up one of these two links and plot its PRRs over time in Figure 13. From Figure 13, we compare the PRRs of this link when it works in Uniform and ATPC. This link quality maintained by this static transmission power level is much more vulnerable to environmental changes. After the first 12 hours, the PRR of the link with static transmission power in Uniform drops dramatically, and it is above 95% PRR only 25% of the time. On the other hand, the same link with ATPC constantly achieves above 99% PRR while exposed in the same environment and using the same radio hardware. These two weak links are between leaf nodes and first-level parent nodes, so the packet loss they caused does not have a big impact on the average end-to-end PRR. However, if such a static transmission power level is used at links with more traffic, such as a link between a two-level parent and the base, the end-to-end communication quality would drop severely.

The Nonuniform solution has weak performance over time. All the links in this solution are vulnerable to link quality variation. However, in the short term and in

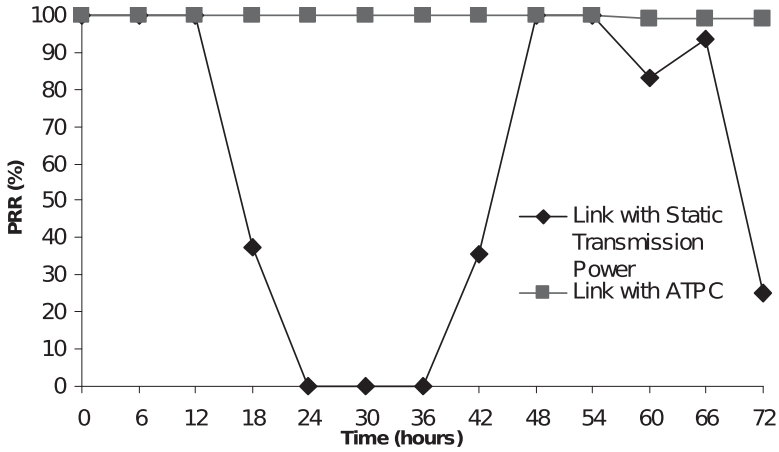

Fig. 13. Link quality.

relatively static weather conditions, Nonuniform can achieve more than 99% end-to-end PRR, as shown in Figure 12. After the first 12 hours, the communication quality of Nonuniform becomes poor and unstable. We also notice that the variation of its trend is much bigger than other solutions. It means the end-to-end PRR with these static transmission power levels at certain time periods can be significantly better or worse than at other time periods of the day. This observation confirms our judgment that the dynamics of link quality may make communication performance unstable and unpredictable when assuming static transmission power.

Considering the quality of wireless communication, ATPC and maximum transmission power solutions are proper to apply in real systems.

4.2.3. Power Consumption. The total energy consumption of the network is measured in the radio's transmission mode when different schemes are used. We calculate the total energy spent in the transmit state of the system by the following formula:

$$E = \sum_{i=1}^{n} \sum_{j=min}^{max} (NumD_{ij} \times TE_j \times LD + NumC_i \times maxTE \times LC), \tag{16}$$

where i is the node ID and j is the transmission power level. $NumD_{ij}$ is the number of data packets sent at node i with transmission power level j. TE_j is the transmission energy consumed per bit from ChipconCC2420 [2005]. LD is the length of a data packet, which is 45 bytes. All the control packets are sent with the maximum transmission power level. $NumC_i$ is the number of control packets (beacons and notifications) sent at node i. $maxTE$ is the transmission energy per bit when using the maximum transmission power level. We get $maxTE$ also from ChipconCC2420 [2005]. LC is the length of a control packet, which is 19 bytes. In our experiments, the ratio of the number of control packets and the number of data packets is 3.9%. The ratio of the energy consumed by control packets and the energy consumed by data packets is 1.9%. ATPC achieves energy-efficient transmission with small control overhead.

For better comparison, we take the energy consumption of the Max scheme as the baseline, which is unit 1 in Figure 14. The power consumptions of the other three schemes are represented as percentage values compared with this baseline. The empirical data demonstrate that ATPC and Nonuniform consume the least transmission energy. Considering that ATPC has much better communication quality than

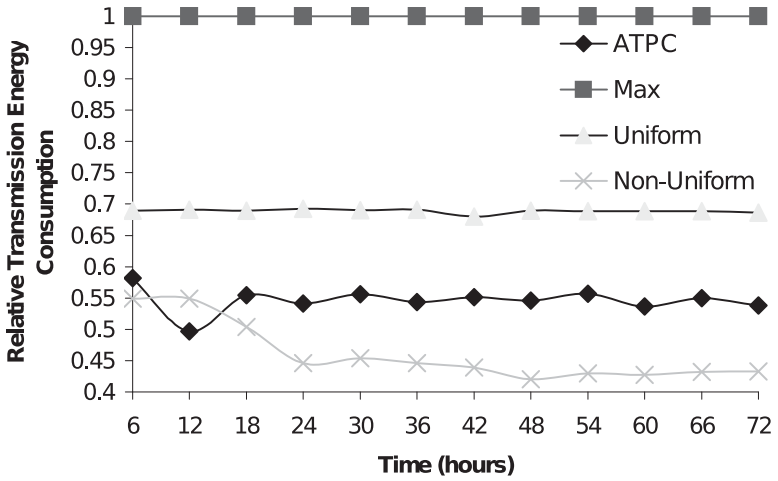

Fig. 14. Transmission power consumption over time.

Nonuniform, ATPC is the most energy-efficient solution. In Figure 14, ATPC has much less transmission energy consumption than Max and Uniform. Although ATPC has extra beacon and feedback packets, the average transmission energy consumption of ATPC is about 53.6% of Max and 78.8% of Uniform.

The trend of ATPC's energy consumption varies a little bit. The main factor causing this variation is the transmission power level variation. There are only three feedback packets per link per day on average. Comparing ATPC with Nonuniform in the first 6 hours, ATPC has similar energy consumption as Nonuniform. The reason is that the transmission power level of each mote does not change much in the first 6 hours. In the next 6 hours, Nonuniform has higher energy consumption than ATPC because a large number of nodes decrease their transmission power level to save energy in ATPC. Later, the transmission energy of Nonuniform drops mainly because of its low PRR, which reduces the number of transmission relays.

Max and Uniform have relatively stable transmission energy consumptions because they use a static transmission power level and their network throughput is stable. The transmission power level used in Uniform largely depends on the topology. In a network with long-distance neighbors, this uniform transmission power level tends to get close to the maximum transmission power level. Both solutions waste significant transmission energy compared to ATPC.

The total energy consumption of Nonuniform varies because its network throughput varies. Compared to the other solutions, it consumes the least transmission energy over time. It doesn't have the overhead of feedback in ATPC, but the energy is not used efficiently due to its low communication quality. However, it may provide good communication quality and save energy in the short term.

We choose three links and plot the average transmission power they used over time in Figure 15. All these links constantly have above 98% PRR. From Figure 15, we have two main observations as follows.

From a historical record of the tuning process in ATPC, it is confirmed that link qualities vary significantly in reality. Though all these links work in the same environment, the tuning rate and range of transmission power for different links can be significantly different. We can see that Link A has a large varying range, which means high sensitivity to environmental changes. The transmission power of Link C is quite stable; it is

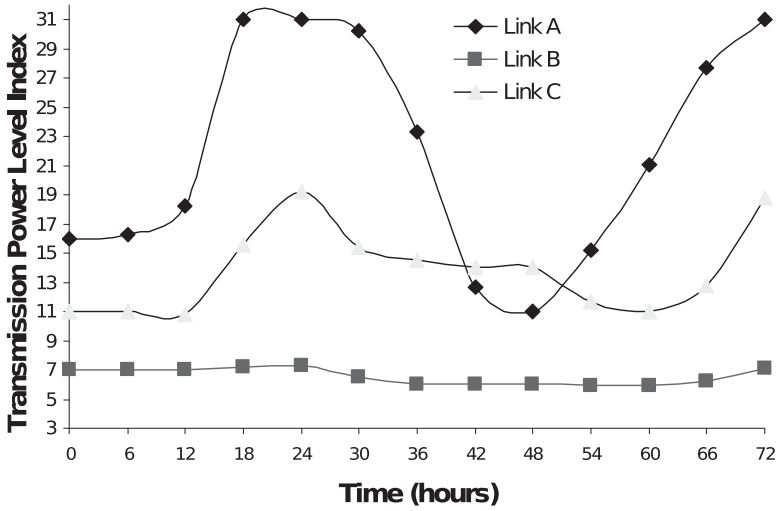

Fig. 15. Average transmission power level over time.

a robust link to environmental changes. The variation of transmission power of Link B is in between. Link B is a more typical case in our experiments.

ATPC is robust in handling dynamics of link quality in reality, according to differences of link conditions. Although all these links are exposed to the same environment, the impacts of the environment on them are link specific. ATPC successfully adjusts the transmission power differently. It also confirms our judgments in Section 2.3.2 both that environmental change is a major reason for the transmission power adjustment and that the adjustment speed depends on the variation speed of the environment.

To summarize, ATPC maintains above 98% end-to-end communication quality while saving transmission power significantly. The static nonuniform transmission power solution may work well on the short term in static environments, but its communication qualities are very vulnerable to environmental changes. The maximum transmission power solution is robust with regard to environmental changes but wastes transmission energy.

5. STATE OF THE ART

There are three categories of research topics related to our ATPC: Transmission Power Control, Topology Control, and empirical studies on wireless radio communication.

There is a small amount of research on realistic transmission power control for wireless sensor networks. The authors of Son et al. [2004] provide a valuable study about the impact of transmission power control on link qualities and propose a novel blacklisting approach. The ATPC we propose is different from their work. First, since link quality varies with time, different transmission powers are needed to maintain the same desired link quality. ATPC uses a feedback-based scheme to pick optimal power levels at different times; this is not addressed in Son et al. [2004]. Second, the protocol in Son et al. [2004] fixes the number of configurable power levels, reducing the design flexibility and also limiting the maximum power tuning accuracy that can be achieved. Also, Jeong et al. [2007] make an experimental comparison of several existing transmission power control algorithms, and Heidemann and Ye [2004] give a short survey of transmission power control. Fu et al. [2012] proposed a PID control-based solution to adjust transmission power. Lee and Chung [2011] investigate the impact

of temperature on power control and propose a temperature-aware power adjustment scheme.

There is some other work on transmission power control evaluated in simulation. Ramanathan and R-Hain [2000] formulate the transmission power adjustment problem for static and dynamic network topologies. Wattenhofer et al. [2001] describe a power control algorithm to increase transmission power to reach neighbors. The protocol in Narayanaswamy et al. [2002] introduces cluster-based transmission power control. Li et al. [2005] propose an algorithm that increases transmission power to reach neighbors in every cone of a certain degree. In Sabitha and Thyagarajan [2012], a fuzzy-logic-based transmission power control design is introduced. Xing et al. [2009] consider transmission scheduling and power control optimization. Cotuk et al. [2014] investigate the impact of different power control strategies on network lifetime. Valli and Dananjayan [2010] introduce a good theory-based power control scheme. Zhu et al. [2012] study event detection in power-controlled and duty-cycled sensor networks. Most of these works are simulation based and they ignore the in situ impact on communication quality in reality. Our approach is based on systematic empirical studies, and we adopt a unique feedback-based approach, tuning link quality pairwise.

Topology control research is a well-studied area in ad hoc and sensor network communities. The goal of a significant portion of these efforts is to achieve better network performance, considering throughput, connectivity, network size, traffic load, and so on. These works can be classified in three major categories according to the transmission range and power assumptions: network-level uniform transmission power [Park and Sivakumar 2002b; Narayanaswamy et al. 2002; Bettstetter 2002; Kirousis et al. 2000; Santi and Blough 2003], node-level nonuniform transmission power [Gomez and Campbell 2004; Bettstetter 2002; Kirousis et al. 2000; Kubisch et al. 2003; Ramanathan and R-Hain 2000; Wattenhofer et al. 2001; Kawadia et al. 2001; Park and Sivakumar 2002a; Rodoplu and Meng 1999; Li et al. 2002], and neighbor-level transmission power solutions [Liu and Li 2002; Xue and Kumar 2004; Blough et al. 2003]. Most of these works are based on simulations, which carry the assumptions that the transmission range is static and circular and that within the transmission range the link quality is perfect and never changes. However, such assumptions do not hold in reality. Therefore, solutions making these assumptions may lead to unstable and unpredictable communication qualities. ATPC, based on empirical studies about communication reality, addresses the practical issues of radio and link dynamics.

There are a number of experimental research results on radio communication reality in wireless sensor networks. Hackmann et al. [2008] investigate different link quality metrics for power control in indoor environments. Srinivasan et al. [2010] present empirical studies of wireless sensor network performances in the home environment. In Chipara et al. [2010], hospital wireless experimental results are presented. Feng et al. [2013] investigate the beamforming scheduling algorithm and related power control issues. Ganesan et al. [2002], Woo et al. [2003], and Jeong et al. [2007] extensively study communication reality in a large-scale sensor network. Zhao and Govindan [2003] study the impact of spatial-temporal characteristics on packet loss and its environmental dependence on packet delivery performance in a wireless sensor network. Zhou et al. [2004, 2011] give a lot of insight on causes of the link quality variations. Park et al. [2010] study the impacts of key parameters in the medium access control layer on energy consumption of the network. Reijers et al. [2004] suggest using the RSSI value as a reliable parameter to predict a reception rate. Lal et al. [2003] study the relationship between SNR and PRR. With different foci, these experimental works are complementary to our work.

Although the literature is rich, simplifying assumptions may hinder most work from being applied directly to physically deployed sensor networks. We believe a practical

transmission power control algorithm like ATPC is the key to apply previous theoretical work to real-world wireless sensor networks.

6. CONCLUSIONS AND FUTURE WORK

We believe there is a serious gap between existing theory work and in situ practice. As a solid step toward the in situ topology control in sensor networks, ATPC presents a lightweight transmission power control technique in a pairwise manner. This fine-granularity tuning trades off computation and local memory (e.g., needing a table in each node) with communication, a much more costly operation in terms of energy. Our in situ experiments reveal the correlation between RSSI/LQI and link quality. Such observations guide us to set up a model to predict the proper transmission power, which is enough to guarantee a good packet reception ratio. We acknowledge that this work is by no means conclusive. However, it indicates a worthwhile direction for future research, so that we can build sensor systems for practical deployment.

Our experiments are designed without congestion and collision. According to our experimental results, ATPC works very well in TDMA protocols. In a low utilization network, where collision and congestion do not happen very frequently, ATPC can still work well. This is because feedback control is renowned for its ability to handle stochastic disturbances.

Conflicting transmissions and interferences may impact the performance of ATPC. However, the capture effect makes the influence of collision and interference on ATPC less serious. Since a packet can be received even when there are overlapped radio signals raised by simultaneous transmission, using RSSI/LQI of such a packet may drive ATPC to an unsteady state. Whitehouse et al. [2005] address a technique to detect packet collision. Zhou et al. [2005] create an approach to detect interferences. By adopting such techniques, RSSI/LQI for packets identified from packet collision is not considered as input for ATPC. Therefore, ATPC is expected to work equally well in a CSMA network by filtering disturbances caused by collision and interference. This is one of the major future works for ATPC.

REFERENCES

A. Arora, P. Dutta, S. Bapat, V. Kulathumani, H. Zhang, V. Naik, V. Mittal, H. Cao, M. Demirbas, M. Gouda, Y. Choi, T. Herman, S. Kulkarni, U. Arumugam, M. Nesterenko, A. Vora, and M. Miyashita. 2004. A line in the sand: A wireless sensor network for target detection, classification, and tracking. *Comput. Networks* 46, 5 (2004), 605–634.

P. Asare, D. Cong, S. G. Vattam, B. Kim, A. L. King, O. Sokolsky, I. Lee, S. Lin, and M. Mullen-Fortino. 2012. The medical device dongle: An open-source standards-based platform for interoperable medical device connectivity. In *ACM IHI*.

C. Bettstetter. 2002. On the connectivity of wireless multihop networks with homogeneous and inhomogeneous range assignment. In *IEEE VTC*.

D. Blough, M. Leoncini, G. Resta, and P. Santi. 2003. The k-neigh protocol for symmetric topology control in Ad Hoc networks. In *ACM MobiHoc*. 141–152.

A. Cerpa, J. L. Wong, L. Kuang, M. Potkonjak, and D. Estrin. 2005. Statistical model of lossy links in wireless sensor networks. In *ACM/IEEE IPSN*.

O. Chipara, Z. He, G. Xing, Q. Chen, X. Wang, C. Lu, J. Stankovic, and T. Abdelzaher. 2006. Real-time power aware routing in wireless sensor networks. In *IWQOS*.

O. Chipara, C. Lu, T. C. Bailey, and G-C. Roman. 2010. Reliable clinical monitoring using wireless sensor networks: Experiences in a step-down hospital unit. In *Proceedings of the 8th ACM Conference on Embedded Networked Sensor Systems (SenSys'10)*.

ChipconCC1000. 2005. CC1000 A unique UHF RF Transceiver. Retrieved from http://www.chipcon.com.

ChipconCC2420. 2005. CC2420 2.4 GHz IEEE 802.15.4/ZigBee-ready RF Transceiver. Retrieved from http://www.chipcon.com.

H. Cotuk, K. Bicakci, B. Tavli, and E. Uzun. 2014. The impact of transmission power control strategies on lifetime of wireless sensor networks. *IEEE Trans. Comput*. 63, 11 (Nov. 2014), 2866–2879.

CROSSBOW. 2004. XBOW MICAz Mote Specifications. Retrieved from http://www.xbow.com.

J. Feng, Y. Lu, B. Jung, D. Peroulis, and Y. C. Hu. 2013. Energy-efficient data dissemination using beamforming in wireless sensor networks. *ACM Trans. Sen. Netw.* 9, 3, Article 31 (June 2013), 30 pages.

Y. Fu, M. Sha, G. Hackmann, and C. Lu. 2012. Practical control of transmission power for wireless sensor networks. In *Proceedings of the 2012 20th IEEE International Conference on Network Protocols (ICNP'12)*.

D. Ganesan, R. Govindan, S. Shenker, and D. Estrin. 2001. Highly-resilient, energy-efficient multipath routing in wireless sensor networks. In *ACM Mobile Computing and Communications Review*, Vol. 5.

D. Ganesan, B. Krishnamachari, A. Woo, D. Culler, D. Estrin, and S. Wicker. 2002. Complex behavior at scale: An experimental study of low-power wireless sensor networks. In *Technical Report UCLA/CSD-TR 02-0013*.

J. Gomez and A. Campbell. 2004. A case for variable-range transmission power control in wireless multihop networks. In *IEEE INFOCOM*, Vol. 3. 1425–1436.

J. Gomez, A. Campbell, M. Naghshineh, and C. Bisdikian. 2003. PARO: Supporting dynamic power controlled routing in wireless Ad Hoc networks. In *ACM/Kluwer WINET*, Vol. 9. 443–460.

G. Hackmann, O. Chipara, and C. Lu. 2008. Robust topology control for indoor wireless sensor networks. In *Proceedings of the 6th ACM Conference on Embedded Network Sensor Systems*.

T. He, S. Krishnamurthy, J. A. Stankovic, T. F. Abdelzaher, L. Luo, R. Stoleru, T. Yan, L. Gu, J. Hui, and B. Krogh. 2004. Energy-efficient surveillance system using wireless sensor networks. In *ACM MobiSys*. 270–283.

T. He, J. A. Stankovic, C. Lu, and T. Abdelzaher. 2003. SPEED: A stateless protocol for real-time communication in sensor networks. In *Proceedings of the 23rd International Conference on Distributed Computing Systems (ICDCS'03)*.

J. Heidemann and W. Ye. 2004. Energy conservation in sensor networks at the link and network layers. In *Technical Report USC/ISI-TR-2004-599*.

IEEE 802.15.4 1999. IEEE 802.15.4, Wireless Medium Access Control (MAC) and Physical Layer (PHY) Specifications for Low Rate Wireless Personal Area Networks (LR-WPANs). (1999). IEEE Std. 802.15.4, 2003.

J. Jeong, D. Culler, and J.-H. Oh. 2007. Empirical analysis of transmission power control algorithms for wireless sensor networks. In *Proceedings of the 4th International Conference on Networked Sensing Systems, 2007 (INSS'07)*..

E.-S. Jung and N. H. Vaidya. 2002. A power control MAC protocol for Ad Hoc networks. In *Proceedings of the 8th Annual International Conference on Mobile Computing and Networking (MobiCom'02)*.

V. Kawadia, S. Narayanaswamy, R. S. Sreenivas, R. Rozovsky, and P. R. Kumar. 2001. Protocols for media access control and power control in wireless networks. In *Proceedings of the 40th IEEE Conference on Decision and Control*. 1935–1940.

L. M. Kirousis, E. Kranakis, D. Krizanc, and A. Pelc. 2000. Power consumption in packet radio networks. In *Theoretical Computer Science*, Vol. 243. 289–305.

M. Kubisch, H. Karl, A. Wolisz, L. C. Zhong, and J. M. Rabaey. 2003. Distributed algorithms for transmission power control in wireless sensor networks. In *IEEE WCNC*.

D. Lal, A. Manjeshwar, F. Herrmann, E. Uysal-Biyikoglu, and A. Keshavarzian. 2003. Measurement and characterization of link quality metrics in energy constrained wireless sensor networks. In *IEEE GlobeCom*, Vol. 1. 446–452.

J. Lee and K. Chung. 2011. An efficient transmission power control scheme for temperature variation in wireless sensor networks. *Sensors* 11, 3, 3078–3093.

L. Li, J. Halpern, V. Bahl, Y. M. Wang, and R. Wattenhofer. 2005. A cone-based distributed topology-control algorithm for wireless multi-hop networks. *IEEE/ACM Trans. Networking* 13, 147–159.

X. Y. Li, P. J. Wan, Y. Wang, and O. Frieder. 2002. Sparse power efficient topology for wireless networks. In *HICSS*.

S. Lin, T. He, and J. A. Stankovic. 2008. CPS-IP: Cyber physical systems interconnection protocol. *SIGBED Rev.* 5, 1, Article 22 (Jan. 2008), 2 pages.

S. Lin, G. Zhou, K. Whitehouse, Y. Wu, J. A. Stankovic, and T. He. 2009. Towards stable network performance in wireless sensor networks. In *Proceedings of the 2009 30th IEEE Real-Time Systems Symposium (RTSS'09)*.

H. Liu, J. Li, Z. Xie, S. Lin, K. Whitehouse, J. A. Stankovic, and D. Siu. 2010. Automatic and robust breadcrumb system deployment for indoor firefighter applications. In *Proceedings of the 8th International Conference on Mobile Systems, Applications, and Services*.

J. Liu and B. Li. 2002. MobileGrid: Capacity-aware topology control in mobile Ad Hoc networks. In *IEEE ICCCN*. 570–574.

J. Liu, J. Reich, and F. Zhao. 2003. Collaborative in-network processing for target tracking. *EURASIP JASP* 4 (April 2003), 378–391.

S. Narayanaswamy, V. Kawadia, R. S. Sreenivas, and P. R. Kumar. 2002. Power control in Ad Hoc networks: Theory, architecture, algorithm and implementation of the COMPOW protocol. In *Proceedings of the European Wireless Conference*. 156–162.

P. Park, C. Fischione, and K. H. Johansson. 2010. Adaptive IEEE 802.15.4 protocol for energy efficient, reliable and timely communications. In *Proceedings of the 9th ACM/IEEE International Conference on Information Processing in Sensor Networks*.

S. J. Park and R. Sivakumar. 2002a. Load-sensitive transmission power control in wireless ad-hoc networks. In *IEEE GlobeCom*, Vol. 1. 42–46.

S. J. Park and R. Sivakumar. 2002b. Quantitative analysis of transmission power control in wireless ad-hoc networks. In *IWAHN*. 56–63.

R. Ramanathan and R. R-Hain. 2000. Topology control of multihop wireless networks using transmit power adjustment. In *IEEE INFOCOM*, Vol. 2. 404–413.

N. Reijers, G. Halkes, and K. Langendoen. 2004. Link layer measurements in sensor networks. In *IEEE MASS*. 224–234.

V. Rodoplu and T. H. Meng. 1999. Minimum energy mobile wireless networks. In *IEEE JSAC*, Vol. 17. 1333–1344.

R. Sabitha and T. Thyagarajan. 2012. Fuzzy logic-based transmission power control algorithm for energy efficient MAC protocol in wireless sensor networks. *Int. J. Commun. Netw. Distrib. Syst.* 9, 3/4 (Aug. 2012), 247–265.

P. Santi and D. M. Blough. 2003. The critical transmitting range for connectivity in sparse wireless ad hoc networks. *IEEE Trans. Mobile Comput.* 2, 25–39.

S. K. Sarkar, T. G. Basavaraju, and C. Puttamadappa. 2007. *Ad Hoc Mobile Wireless Networks: Principles, Protocols and Applications*(1st ed.). Auerbach Publications, Boston, MA, USA.

P. M. Shankar. 2001. *Introduction to Wireless Systems*. John Wiley and Sons.

S. Singh, M. Woo, and C. S. Raghavendra. 1998. Power-aware routing in mobile ad hoc networks. In *ACM MobiCom*. 181–190.

D. Son, B. Krishnamachari, and J. Heidemann. 2004. Experimental study of the effects of transmission power control and blacklisting in wireless sensor networks. In *IEEE SECON*. 289–298.

K. Srinivasan, P. Dutta, A. Tavakoli, and P. Levis. 2010. An empirical study of low-power wireless. *ACM Trans. Sen. Netw.* (2010).

J. A. Stankovic, Q. Cao, T. Doan, L. Fang, Z. He, R. Kiran, S. Lin, S. Son, R. Stoleru, and A. Wood. 2005. Wireless sensor networks for in-home healthcare: Potential and challenges. In *HCMDSS*.

M. W. Subbarao. 1999. Dynamic power-conscious routing for MANETs: An initial approach. In *IEEE VTC*. 1232–1237.

G. Tolle, J. Polastre, R. Szewczyk, N. Turner, K. Tu, S. Burgess, D. Gay, P. Buonadonna, W. Hong, T. Dawson, and D. Culler. 2005. A macroscope in the redwoods. In *ACM SenSys*.

D. Tse and P. Viswanath. 2005. *Fundamentals of Wireless Communication*. Cambridge University Press, New York, NY, USA.

R. Valli and P. Dananjayan. 2010. A Non-Cooperative Game Theoretical Approach for Power Control in Virtual MIMO Wireless Sensor Network. *CoRR, abs/1007.5168 (2010)*.

R. Wattenhofer, L. Li, P. Bahl, and Y. M. Wang. 2001. Distributed topology control for power efficient operation in multihop wireless ad hoc networks. In *IEEE INFOCOM*. 1388–1397.

G. Werner-Allen, K. Lorincz, M. C. Ruiz, O. Marcillo, J. B. Johnson, J. M. Lees, and M. Welsh. 2006. Deploying a wireless sensor network on an active volcano. *IEEE Internet Comput*. 10, 18–25.

K. Whitehouse, A. Woo, F. Jiang, J. Polastre, and D. Culler. 2005. Exploiting the capture effect for collision detection and recovery. In *IEEE EmNetS-II*.

A. Woo, T. Tong, and D. Culler. 2003. Taming the underlying challenges of reliable multihop routing in sensor networks. In *ACM SenSys*.

G. Xing, M. Sha, G. Hackmann, K. Klues, O. Chipara, and C. Lu. 2009. Towards unified radio power management for wireless sensor networks. *Wireless Communications and Mobile Computing* (2009).

N. Xu, S. Rangwala, K. K. Chintalapudi, D. Ganesan, A. Broad, R. Govindan, and D. Estrin. 2004. A wireless sensor network for structural monitoring. In *ACM SenSys*.

F. Xue and P. R. Kumar. 2004. The number of neighbors needed for connectivity of wireless networks. *Wireless Networks* 10, 169–181.

J. Zhao and R. Govindan. 2003. Understanding packet delivery performance in dense wireless sensor networks. In *ACM SenSys*.

G. Zhou, T. He, S. Krishnamurthy, and J. A. Stankovic. 2004. Impact of radio irregularity on wireless sensor networks. In *ACM MobiSys*. 125–138.

G. Zhou, T. He, J. A. Stankovic, and T. F. Abdelzaher. 2005. RID: Radio interference detection in wireless sensor networks. In *IEEE INFOCOM*, Vol. 2. 891–901.

G. Zhou, Q. Li, J. Li, Y. Wu, S. Lin, J. Lu, C. Wan, M. D. Yarvis, and J. A. Stankovic. 2011. Adaptive and radio-agnostic QoS for body sensor networks. *ACM Trans. Embed. Comput. Syst*. 10, 4, Article 48 (Nov. 2011), 34 pages.

Y. Zhu, Y. Liu, and L. M. Ni. 2012. Optimizing event detection in low duty-cycled sensor networks. *Wirel. Netw.* 18, 3 (April 2012), 241–255.

Received August 2014; revised December 2014; accepted March 2015